MODELLING CAPILLARY EFFECTS ON THE REACTIVE TRANSPORT OF CHLORIDE IONS IN CEMENTITIOUS MATERIALS

Sanchez, T.[1], Laferriere F.[2], Sorelli, L.[1] and Conciatori, D.[1*]

[1] Laval University, Canada

[2] Lombardi SA, Switzerland

[*] david.conciatori@gci.ulaval.ca

Abstract: The transport of chloride ions in concrete structures is not only due to diffusion but also to the advective effects of water movements and capillarity, mostly present with wet-dry cycles. These last two phenomena are currently very poorly modelled. A new system based on optical fibres was previously developed to measure the free chloride concentration in the pore solution without damaging the material. This work aims at developing a numerical model simulating the reactive transport of chloride ions by capillarity in a cementitious material, which considers the diffusion of chloride ions and water transport by capillarity, as well as the chloride adsorption by the material with chemical interaction. It led to the analysis of the main phenomena occurring during a capillarity test. In a larger perspective, this study improves the current understanding of the durability of concrete structures exposed to severe environmental conditions.

Keywords: Chloride, concrete, numerical model, optical fibre sensor, PhreeqC

1 INTRODUCTION

In western world countries, many existing reinforced concrete structures are deteriorating as they are approaching the end of their expected lifespan. The corrosion of steel rebars is the main cause of damage and early failure in reinforced concrete structures [1,2]. The source of chlorides ions comes from de-icing salts or seawater in littoral zones. The high costs involved in structures maintenance justifies new methods

to predict the degradation and bring about preventive repairs [3]. Surprisingly, some of these structures have been damaged only a few years after having being repaired [4].

It exists several methods for corrosion detection and for chloride detection in reinforced concrete [5,6], which can be categorized as destructive and non-destructive methods. The most destructive method commonly used is the ASTM C1524-02a standard: core drills are extracted from the structure to obtain the chloride penetration depth. The chloride concentration profiles are then obtained following the ASTM C1152/C-1152M and C1218/C-1218M methods. This procedure has the disadvantage of providing inaccurate results as an extremely low amount of chloride content is extracted. It also only provides information on chloride concentration and not on corrosion. Besides, non-destructive methods can provide a quantitative indication of the corrosion propagation [7], but they do not provide a precise indication on the chloride content in the concrete. Other non-destructive methods, such as ASTM C876, can determine the corrosion initiation but their results interpretation suffers from electromagnetic interferences and each test is rather time-consuming (e.g. weeks) [8].

Lately, a non-destructive method applicable in-situ was developed to monitor weak free-chloride concentrations moving through the concrete porosity [9,10]. Over the past ten years, Optical Fibres (OF) have been mainly used for structural health monitoring to measure deformations, vibrations, and strains [11–13]. Those sensors are also employed in fields such as environment, space, automobile, medicine or biochemistry [14] to detect, in-situ, chemicals in a reversible and non-invasive manner [15]. This technology has been recently adapted for monitoring invasive and harmful chemicals in concrete structures for corrosion monitoring [16]. Such new sensors provide an accurate knowledge of chloride concentration at the steel rebar level allowing new opportunities for comparisons with model predictions. Moreover, optical fibres have long lifespans, good mechanical and chemical resistance in concrete, no temperature effects, resilience to electromagnetic influences and high data transfer capacities.

Chloride OF sensors were embedded within the cementitious matrix at 20 mm from the surface and used in the laboratory with a capillarity test in order to observe the free chloride content evolution in the pore solution at a given penetration depth (20 mm) [16,17]. The OF sensors overcame the difficulty encountered

in measuring the capillary suction with the actual experimental methods previously described because they only provided the chloride concentration according to the penetration depth at a given time after grinding the sample. Then, to obtain the evolution of the chloride profile over time with those methods, it is necessary to carry out several capillary tests under the same experimental conditions but of different duration.

The measurements of the capillarity test were subsequently simulated by the software TransChlor [18], which considers the coupling between temperature, carbonation, water transport, ionic diffusion transport [19] and chloride adsorption with interaction isotherms [20]. Its database was created from data available in literature and additional tests carried out on similar material [19]. However, the simulation did not fit the measurements with accuracy in the early days and did not allow the analysis of the influence of each phenomenon (geometrical effects, chemical reactions, etc.) in order to better understand the physics behind.

The presented results first clearly identified the significant role of the chemical interactions which have not been yet considered by the previous numerical models, in the very specific case of a capillarity test. Then, a new numerical model on the geochemical software PhreeqC was developed step-by-step to consider the advection/dispersion transport of water, the chloride diffusion, the chemical reactions (and particularly the chloride adsorption by the cement matrix) and the effects of the capillary pressure (Figure 1). The reliable interpretation of the phenomena in the capillarity test permitted the prediction of the future behaviour of the chloride transport after the end of the test.

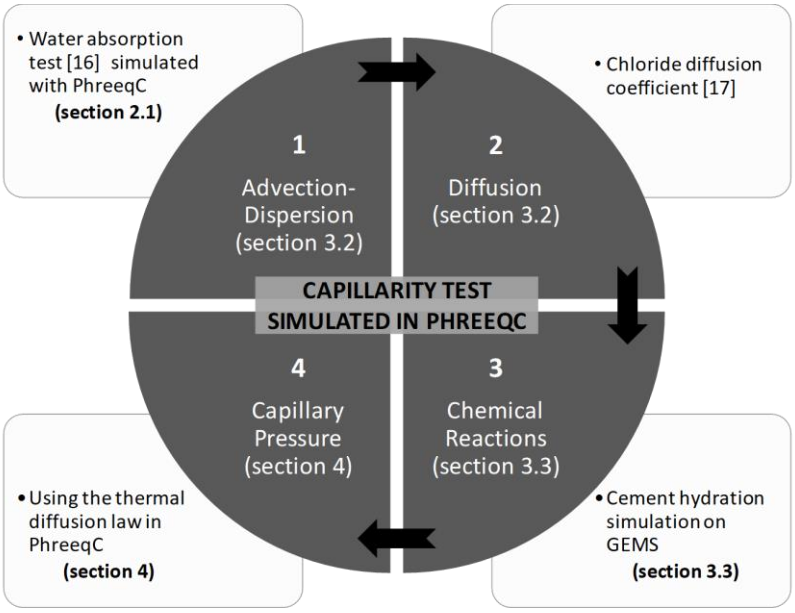

Figure 1. Summary of the modelling strategy to simulate the capillarity test in PhreeqC. The steps are in the black boxes and the references used or the simulations done on other models are in the white boxes.

2 EXPERIMENTAL METHODS AND NUMERICAL MODELS

2.1 Material and characterization

Mix. Cement type CEM I 42.5 (W/C = 0.52) was used with a cement content τ_{Ciment}= 375 kg/m³. The maximum diameter of the aggregate was 16 mm. The aggregate content and the density of hardened concrete value were 1813 kg/m³ and 2384 kg/m³ respectively. The curing was carried out in a controlled room at 23°C (or 73.4°F) with a relative humidity of 100% for 7 days. The class of concrete mixed is C40/50 according to the European code designation [21]. The effective chloride diffusion (D_{Cl}) for this kind of material was previously measured at 5.73×10^{-12} m²/s by D. Conciatori et al. [17].

Water absorption tests were carried out by D. Conciatori [22] on 5 cylindric samples of 50 mm of diameter and 30 mm of length. The test procedure was based on the standard DIN 52617. The samples were dried for 164 days at 23°C and 60% RH to reduce the sample saturation to 75 %. The relative humidity was controlled by a solution with 6.16 mol/l NaCl. The bottom faces of the samples were then exposed to water

for the water absorption test. The evolution of the water content was then observed during the absorption by mass measurements.

In this paper, two numerical models on PhreeqC were created to calibrate the water movement parameters:

- a simple advection model considering a water flux moving in the sample;
- an advection-dispersion model considering further the microstructure geometry.

The evolution of the percentage of water in the porosity was computed from the geometrical characteristics (dimensions and water porosity ∅= 12.99% [17]) of the material (Figure 2). The advection transport model was fitted on PhreeqC with a constant water velocity v_{H2O}= 1.43 mm/h determined by the slope of the curve at the first stage of the absorption test. The numerical model is used to determine an initial water content at 75% (the sample was dried at 75% RH). However, a simple advective model did not generate an accurate reproduction of the evolution of the water in the porosity during the second stage of the transient state (after 10 hours). Indeed, the experimental curve showed a smooth increase of water due to the tortuosity of the pore network. The complexity of the microstructure was then represented by a dispersion parameter α_L= 5 mm in the simulations with the Advection-Dispersion model.

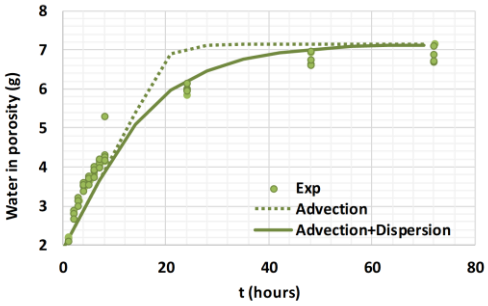

Figure 2 - Evolution of the total water content (%) in the pores network during the water absorption test

OF Chloride sensor [23]**.** The sensor design consists of an optical send (light source blue LED) - receive (spectrometer) module [24] which is connected to the sensor (OPTODE) by optical fibre (Figure 3a) [25,26]. Under the action of the light signal emitted by the source, the transducer emits a fluorescence signal [27,28]. This fluorescence signal is conveyed to the spectrometer by an offset fibre. The light signal is further

converted into an electric signal and analysed by digital electronic processing. The miniaturization of the OPTODE elements allows minimally invasive and in-situ implantation into the thickness of cover concrete. The use of optical fibres permits separation of sensors and spectrometer.

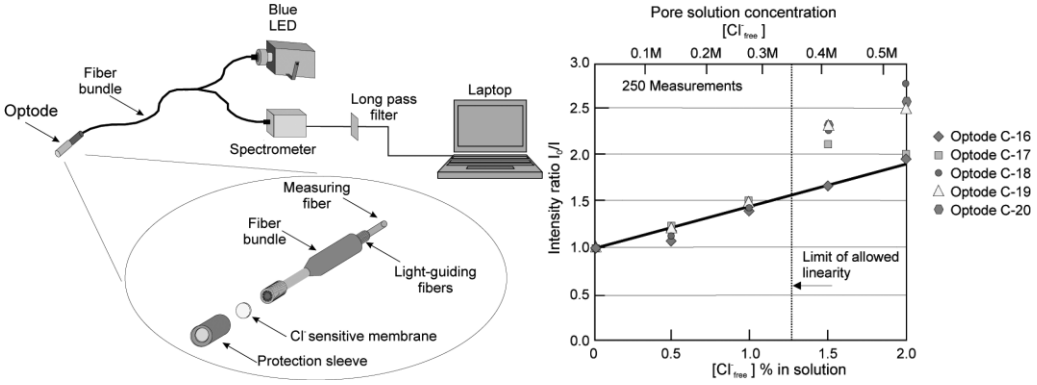

Figure 3. (a) OPTODE instrumental setup and (b) Calibration of the OPTODE sensor [16]

The detection of anionic species, such as chloride ions, requires an indirect method based on fluorescence quenching (reducing in quantum yield) of a reagent caused by its reaction with the analyte [29]. There are many fluorescent molecules (fluorophores) with different excitation and emission wavelengths which can detect the presence of analytes [30]. After preliminary testing and a careful review of environmental and biological studies [31–33], Lucigenin was found to be the best indicator dye [34]. Due to its Sol-gel transparency, mechanical stability, chemical inertia, and flexible configuration. Moreover, the immobilization of the dye by encapsulation is simple and general enough to prevent the leaching of the indicator [35].

The free chloride concentration in the concrete pore solution $[Cl_W^-]$ depends on the fluorescence intensity measured with (I) and without (I_0) chloride ions according to the Stern-Volmer's equation [1]:

$$[Cl_W^-] = 2.2306 \left(\frac{I_0}{I} - 1\right). \quad (1)$$

The calibration curve (Figure 3b) of the Stern-Volmer's equation [1] was carried out against 250 measurements [16]. The I_0/I linearity was verified from 30 mol/m³ (0.1%) to 350 mol/m³ (1.2%) within the calibration range.

2.2 Capillarity test with the chloride sensor

The capillarity test was carried out on a concrete cube of 150x150x150 mm (3.38 10^{-3} m^3) by Laferriere et al. [16]. The chloride sensor was placed at a depth of 20 mm from the bottom surface during the mix (Figure 4a). The sample was then dried at 25°C and 33% RH for 31 days before the test to ensure a saturation of the sample at around 75 % (as for the water absorption test). Afterwards, the lower face of the sample was immersed in a solution of 500 mmol/l NaCl (Figure 4a). In order to induce one-dimensional transport, the four sides of the sample were resin-coated, and the upper face remained in contact with the ambient air. During the test, the temperature and the relative humidity of the climatic chamber were maintained constant at 20°C (68°F) and 80% respectively. The fluorescence intensity measurements were taken every 15 minutes.

After approximately 7 hours, the saline solution reached the OPTODE which started measuring a chloride concentration (Figure 4b). The cure period, which lasted over 31 days in very low moisture conditions, caused an initial rapid absorption when the cube face was exposed to the saline solution at the beginning of the test. The saline solution was hence transported very quickly into the concrete pores.

The maximum concentration was up to 0.65 % cement weight (350 mmol/l) of free chloride ions after 32 hours, then slightly decreased to a value near 0.45 % cement weight (250 mmol/l) before slightly increasing again. The chloride concentrations measured were hence within the limit of the calibration range in between 30 and 350 mol/m^3 confirming the reliability of the results (Figure 4b). Considering the sample volume, the chloride quantity measured in the pore solution can be expressed in percentage of cement weight (g_{Cl^-}/100g_{Cement}), its porosity ∅ and its cement content τ_{Ciment} (kg$_{Cement}$/$m^3_{Concrete}$). The maximal quantity of free chloride ions in the pore solution is constrained by the porosity ∅ of the material and can not exceed $[Cl_W^-]_{Max}$= 0.63 % of cement weight since the chloride concentration upstream was C_0= 513 mol/m^3:

$$[Cl_W^-]_{Max} = \emptyset \frac{C_0 . M_{Cl}}{\tau_{Ciment}}. \quad (2)$$

M_{Cl} is the molar mass of chloride ions (g/mol). This threshold value was reached during the early days. As the temperature and the moisture parameters did not vary during the experiment and the external salt concentration was fixed, the free chloride concentration should stabilize to 0.63% of cement weight at the steady state. However, the concentration decreased after this peak until around 0.45% of cement weight at 7 days. Then, a slow increase of the chloride curve seems to highlight the balancing of the chloride concentrations in upstream and in the pore solution. The concentration of 0.63% of cement weight should then be reached after long time of capillarity tests.

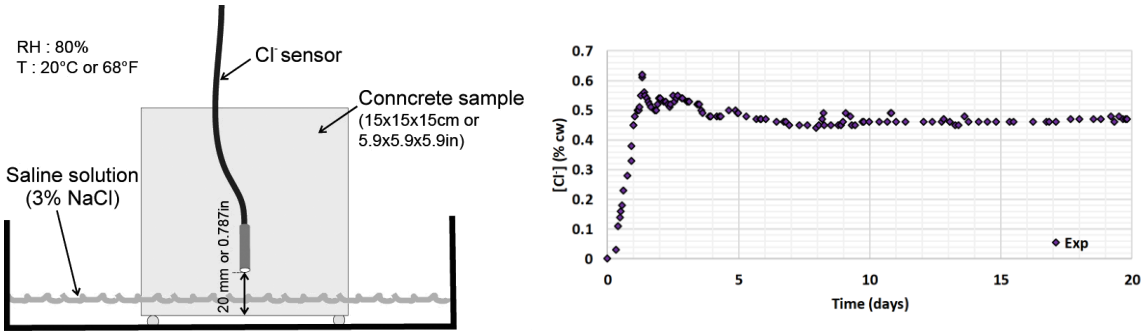

Figure 4. (a) Capillarity test diagram and (b) Free chloride concentration evolution at 20 mm depth

2.3 PhreeqC model

PhreeqC is a freeware developed in C/C++ by Parkhurst and Appelo and well validated in several industrial and academic applications [36,37]. This software allows simulating classical 1D macroscopic transport equations coupled with reactive processes (e.g. [38]) thanks to a chemical database. PhreeqC is also endorsed with a chemical reaction module to simulate the dissolution and precipitation of material solid phase, the oxidation-reduction reactions at the electrodes and the balance between an aqueous phase and the surrounding atmosphere (pure phases, solid solutions, exchange surfaces…). However, various simplifying hypothesis are assumed, such as: (i) the numerical simulation must be based on a large number of experimental test results; (ii) a complete and reliable thermodynamic database (description of ionic species, solid phase…) is necessary for realistic simulations; (iii) and the numerical model is solved using an explicit finite element scheme, which is faster than an implicit one but can be unstable with initial conditions not physically compatible or too large space step (respect Von Neumann criterion [39]).

In this study, we consider that ionic transport takes place in 1D direction under isothermal conditions (T= 20°C at laboratory conditions); the thickness of the sample was sufficiently large to be considered as homogenous. The mass conservation for a chemical species that is transported yields the well-established advection-reaction-dispersion (ARD) equation:

$$\frac{\partial C}{\partial t} = -\mathrm{v_{H2O}}\frac{\partial C}{\partial x} + (D_{Cl} + \alpha_{\mathrm{L}}\mathrm{v_{H2O}})\frac{\partial C^2}{\partial^2 x} - \frac{\partial \mathrm{Q}}{\partial t}. \quad (3)$$

where C is the chloride concentration in water, Q the chloride concentration in the solid phase, D_{Cl} its effective diffusion coefficient and α_{L} the dispersivity (m). The term $\mathrm{v_{H2O}}\frac{\partial C}{\partial x}$ represent the advective transport, $(D_{Cl} + \alpha_{\mathrm{L}}\mathrm{v_{H2O}})\frac{\partial C^2}{\partial^2 x}$ the dispersive transport and $\frac{\partial \mathrm{Q}}{\partial t}$ the chemical reaction with chloride and the solid phase of the material. The water velocity $\mathrm{v_{H2O}}$ is assumed to be constant by PhreeqC for a given time step. The chloride concentration in the solid phase Q [40] is defined by the concentration of an ionic species bound to the surface of the material $c_{s,Cl}$ (mol/kg), the density of the free area ρ_b (kg/L) and the accessible porosity $\emptyset_{Cl}$:

$$Q = \frac{c_{s,Cl}\,\rho_b}{\emptyset_{Cl}}. \quad (4)$$

In the numerical model, the concentration $\mathrm{C}(t + \Delta t)$ of a species i at the time step $(t + \Delta t)$ depend on $C(t)$ as required by an explicit time scheme. The reactive term $\frac{\partial \mathrm{Q}}{\partial t}$ is computed by a decoupled PhreeqC chemical reaction module for more efficiency [41]. Chemical reactions with kinetics are solved with the Range-Kutta method [42] and the chemical reaction time step is automatically subdivided. The iterative Newton-Raphson method [43] is used to find an optimal chemical state (or by an optimization method if chemical reactions are not linearly independent).

3 PRELIMINARY NUMERICAL SIMULATIONS

3.1 Limitation with the TransChlor model

TransChlor is a 1D model intended for saturated and unsaturated concrete. It considers the transport of both water and chloride ions [17–19,22,44]. The water transport is determined by temperature according to the W/C ratio, the relative humidity and depends on the time of contact between concrete and liquid water [45]. The capillarity effect decreases as a function of time representing the saturation of the material and calibrated with experimental tests on similar materials [46]. The chloride transport includes the effects of their ionic diffusion in water and the water advection [47]. The delay of the chloride front compared to the waterfront during the advection movement is modelled by a delay coefficient [46]. The chloride adsorption by the cement phases is considered by using the Freundlich isotherm [48].

The comparison of the measured chloride numerical evolution at a depth of 20 mm with the TransChlor model predictions is shown in Figure 5. The chloride sensor measurements and the model predictions converge at 8 days. However, during the early period of the test, the two curves representing the free chloride content started at different times: the free chloride ingress measured appears earlier at 20 cm. The reasons of this initial discrepancy can have various causes: the delay coefficient included in the TransChlor model (R_{Cl}= 0.7) is not known for this specific type of material but for standard material. One may wonder if the capillarity suction equation [5] is well adapted for this kind of material and test: the water-time exposition t_c could be underestimated. Additionally, it could also come from the difference in the compaction of the sample: parameters used in TransChlor predictions are obtained from a standard concrete vibrated using a needle, whereas the cube sample compaction was carried out by vibration of the formwork in order to minimize the risks of breaking the sensor. After 8 days, the measures seem to slightly increase again maybe due to the limit of adsorption capacity of the material contrary to the TransChlor simulation. As the quantity adsorbed in the model is unlimited, the numerical curve stabilized at around 0.45 %.

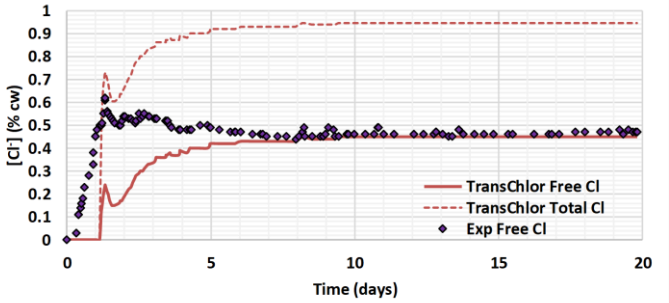

Figure 5. TransChlor simulation of the evolution of free chloride concentration and total chloride concentration at 20mm depth

It can be observed that the measured kinetics of the chloride penetration front at the early test was faster than in the model. In other terms, the concrete cube permeability seems to be higher than envisaged by the model. This measured front was also characterized by a more important peak of the concentration in the pore solution corresponding to 0.63 % of cement weight, the threshold chloride concentration in the pore solution (in view of the material porosity). The most likely hypothesis to explain the difference observed between the two free chloride curves could be the effects of chemical interactions between the chloride ions and the sample solid phase. Indeed, chloride adsorption by the cement matrix could occur after some delay whereas the numerical model considered them from the beginning. TransChlor modelled the chloride interaction with Freundlich isotherms: the total chloride content simulated in the sample with TransChlor is presented (dash line in Figure 5). This curve does not exceed the maximum total chloride content $[Cl^-_{Tot}]_{Max}$ in the concrete sample, which can be estimated to 1.22 % of the cement weight, based on a formula (5) from Vincler et al. [49]:

$$[Cl^-_{Tot}]_{Max} = V_{w/c}\frac{C_0 M_{Cl}}{\tau_{Ciment}}. \quad (5)$$

$V_{w/c} = \tau_{Ciment} * W/C$ ($\mathrm{m^3_{Water}/m^3_{Concrete}}$) represents the volume of water used to cast one cubic meter of concrete. It also appears that the simulated total chloride peaks correspond to the measured free chloride one demonstrating that some effects prevent reactions in the first days.

3.2 Advection-Dispersion model on PhreeqC

A simple Advection-Dispersion model was first developed using the water absorption test data (see 2.1): the water velocity is v_{H2O}= 1.43 mm/h and the dispersion parameter is α_L= 5 mm. The model considered a solution in the upstream of 513 mol/m³ NaCl at 20°C. The upstream boundary was assumed to be constant during the whole test. The concrete sample of 150 mm in length was discretized in 15 cells of 10 mm. Each cell contained an initial water volume corresponding to a sample saturation of 75%. The downstream border is a closed condition. Figure 6a presents the simulation of the free chloride concentration evolution at 20 mm depth, equivalent to the total chloride concentration as no chemical reaction was considered.

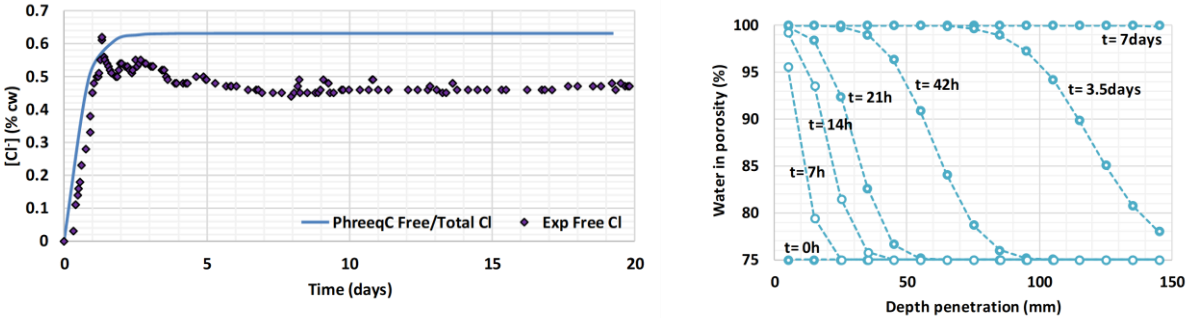

(a) (b)

Figure 6 - Advection-Dispersion simulation of (a) the evolution of free chloride concentration and (b) the evolution of the water content in the porosity (%) according to the penetration depth

The Advection-Dispersion model appropriately simulates the kinetics of the capillarity test at an early age: the parameter defining the water transport, previously obtained in a similar sample appears to fit well. The softening of the curve at 1 day comes from the dispersion that represents the complexity of the pore microstructure. However, the simulation of the steady state is not correct because as the upstream chloride concentration was constant at 513 mol/m³ (corresponding to 0.63 % cement weight in the pore solution), the concentration was also equal at steady state. As for the measured chloride, the free chloride concentration after 1.5 days decreased to 0.5 % of the cement weight (Figure 6a), thus demonstrating the adsorption of the chloride. A more complex model considering the chemical interaction is then needed.

By simulating the water ingress through the pore network, the complete saturation of the sample porosity can be predicted at about 6 days (Figure 6b). At this moment, only ionic diffusion governed the chloride transport. As a first order approximation, the advection-dispersion transport was stopped when the cell was completely filled (at 6 days) and replaced by a diffusion transport. This ensures the mass conservation in the sample and it will be essential when chemical reactions will be considered in a more complex model.

3.3 Advection-Dispersion-Reaction model on PhreeqC

As the experimental tests were done in previous studies, there is no concrete samples left to analyze its chemical composition. That's why, the GEMS software [50] with the Nagra-PSI thermodynamic database [51] was used to simulate the composition of the cement phase for the sample in this work (150x150x150 mm) considering a total hydration (Table 1). The simulation was based on the composition of the main clinker phases of the cement CEM I 42.5 given in [52]. The pH of the pore solution was estimated by GEMS to be 13.52 based on the content of K2O and Na2O in the sample. Monocarbonate is the main phase in the interaction of the chloride ions with the cement matrix.

Table 1. Composition of the hydrated cement part of the sample given by GEMS simulation

Main cement phases	GEMS quantity (g/100g_{cement})
C-S-H	56.04
Portlandite	35.06
Calcite	3.73
Ettringite	16.92
Monocarbonate	3.96
OH-Hydrotalcite	5.13

For the Advection-Dispersion-Reaction (ADR) model in PhreeqC, the chemical reactions were phenomenologically considered using the cement database 'Andra Thermochimie' [53,54] while taking into account the quantity of CSH, Portlandite, Calcite, Ettringite and Monocarbonate in the sample. Friedel salts

can be created by a solid solution mechanism (but they are not initially present) [55]. The Monocarbonate evolution in the model was also governed by the solid solution mechanism [56]. The addition of chemical reactions with chloride ions in the numerical model has created a delay that can be observed on the simulated free chloride curve (continuous line in Figure 7). At steady state, the simulated curve mimics the advection-dispersion curve and reaches the maximal value in the pore solution (0.63 % cement weight).

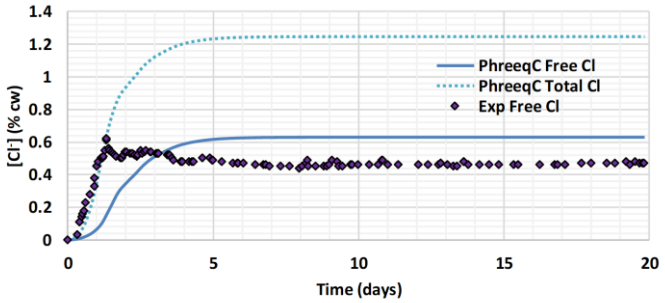

Figure 7 - PhreeqC simulation (ADR) of the evolution of free chloride concentration and total chloride concentration at 20mm depth

The total chloride evolution at 20 mm has also been simulated with the Advection-Dispersion-Reaction model (dashed curve in Figure 7). The maximum total chloride value in the concrete sample (1.22 % of the cement weight) is not exceeded. Contrary to what was expected, it was the simulated total chloride curve that fitted the early state of the free chloride measures. This observation clearly highlights that there is no chloride adsorption in the experiments during the first hours. The chemical reaction kinetic seems to be reduced (or even stopped). The chloride adsorption starts only after 1 days of test, which correspond to the separation of the simulated total chloride and the measured free chloride curves. This delay also coincides with the saturation time of the first 20 mm of the sample. After that, the region surrounding the chloride sensor was totally saturated by water (Figure 6b). An explanation of the reason why chemical reactions seem to be neglected in the first hours could then be the presence of a pressure in the sample due to capillarity effects [57].

4 RESULTS AND DISCUSSIONS

The chloride ingress in the capillarity test was previously modelled by an Advection-Dispersion-Reaction (ADR) transport model on PhreeqC. The analysis of these preliminary numerical simulations does not reproduce accurately the evolution of the chloride concentration in the pore solution as chemical reactions in the experiments seem to be delayed during the saturation period of the sample. This phenomenon could be explained as an effect of the capillary pressure which block the chemical reaction during the first hours (with the advective-dispersive transport). A complete numerical model for the capillarity test needs to consider the capillary pressure during the sample saturation by water.

First, simulations were carried out considering directly a pressure in the pore solution of the PhreeqC model (with the '-pressure' routine). However, it did not yield successful results or any perceptible impact on the chemical reactions mainly because of the rapid and linear evolution of the pressure which does not correspond to the smooth evolution of water in the porosity (dash line in Figure 8a). As a simplified approach, an alternative solution was therefore proposed to disrupt the temperature variable in the PhreeqC model. Indeed, the capillary pressure P_{Cap} can be linked to a 'capillary temperature' T_{Cap} with the perfect gas law at the test conditions (T_0= 20°C, P_0= 1 atm) in the unsaturated pore network of the material:

$$P_{Cap} = \frac{R\rho_{Air}}{M_{Air}} T_{Cap}. \tag{6}$$

ρ_{Air}= 1.204 kg/m³ represents the air density (Dry air, P_0= 1 atm, T_0= 20°C) and the air molar mass is considered M_{Air}= 28.96 g/mol. Originally, the heat transport equation for a chemical substance is:

$$\mathrm{R_T}\frac{\partial T}{\partial t} = -\mathrm{v_{H2O}}\frac{\partial T}{\partial t} + (\kappa + \beta_{\mathrm{L}}\mathrm{v_{H2O}})\frac{\partial^2 T}{\partial x^2} \tag{7}$$

with the temperature retardation factor $\mathrm{R_T}$ depending on the density ρ and the specific heat k [37]:

$$\mathrm{R_T} = 1 + \frac{(1-\emptyset)}{\emptyset}\frac{\rho_s k_s}{\rho_w k_w} \tag{8}$$

The thermal dispersivity β_{L} and the hydrodynamic dispersivity α_{L} are assumed to be equal [58] whereas the thermal diffusion coefficient κ is ten times larger than D. As the temperature test was constantly at T_0= 20°C, the heat transport equation (10)-(11) can be used to describe the 'capillary temperature' T_{Cap} evolution:

$$\mathrm{R}_T \frac{\partial T_{Cap}}{\partial t} = -\mathrm{v}_{\mathrm{H2O}} \frac{\partial T_{Cap}}{\partial t} + (\kappa_T + \alpha_{\mathrm{L}} \mathrm{v}_{\mathrm{H2O}}) \frac{\partial^2 T_{Cap}}{\partial x^2}. \quad (9)$$

α_{L} is the dispersivity coefficient (same as previously stated in the transport equation). The two following parameters were fitted to respect the curves: the retardation factor R_{T}= 3 and the thermal diffusion same as the ionic diffusion (κ_{T}= 1.10^{-12}). As the temperature in the upstream was constant during all the test, we created a temperature gradient between the sample and the upstream solution simulating the depression. The chloride curve was fitted with an evolution of the capillary pressure P_{Cap} varying from 1.6 atm to 1 atm (atmospheric pressure) in the sample (Figure 8a). Then, the initial capillary pressure P_{Cap} in the sample was estimated to twice the atmospheric pressure. The pressure stabilized at 1 atm after 7 days because the diffusion transport replaced the advection-dispersion transport as the sample was totally saturated by water.

PhreeqC simulated the evolution of the different phases in the cement matrix at 20 mm (Figure 8). The pH of the pore solution increased until 13.4 equilibrating the hydroxide concentration with the different phases such as Na_2O and K_2O. In Figure 8b, the simulation of the content evolution of the Portlandite, Calcite and C-S-H can be observed. When the capillary pressure decreases in the sample, the Portlandite and Calcite precipitated to equilibrate the concentration of calcium and aluminum in the pore solution. In Figure 8c, the content evolution of Ettringite, Monocarbonate and Friedel salts were simulated. As Monocarbonate are very sensitive to the pressure in the water, their content increased in the first days with the decrease of the capillary pressure. The precipitation of Ettringite equilibrated the sulphate concentration in the pore solution. When the capillary pressure decreased below 1.15 atm, chloride ions formed Friedel salts. The portlandite precipitated at the same time to release Calcium for Friedel salts formation. Lastly, a very slight evolution of C-S-H was simulated (around 2.10^{-5} mol). PhreeqC equilibrated its content with Calcium at the beginning of the test then it decreased with the Friedel salts formation. The chloride physical binding by C-S-H has

not been considered as it is negligible in a healthy material (C/S rate is larger) [59]. On the 5th day of the test, chemical reactions became negligible as the diffusion transport replaced the advection-dispersion. The water suction hence seems to accelerate the dissolution of cement phases and the decalcification of the cement matrix in the first days of the test due to the ingress of the NaCl solution at pH 7 [60,61].

The free and total chloride contents simulated at 20 mm are given in Figure 8d. The chloride ions were not bound by the cement matrix in the first hours: free and total chloride contents are similar. Whereas when the capillary pressure decreased, the adsorption of chloride increased: the total chloride content increased, and the free chloride decreased. When the diffusion process replaced the advection-dispersion, the total curve stabilized at around 1.2 % of cement weight that is near the maximal value reachable (at 1.22 %). The value of 1.2 % cement weight will be reached at around 120 days according to the PhreeqC prediction. Those predictions also allow to estimate that, during the diffusion transport, the free chloride concentration in the sample will increase again and reach the maximal value of 0.62 % cement weight after 450 years of capillarity test whereas the first prediction with TransChlor estimated the free chloride constantly at 0.45 %.

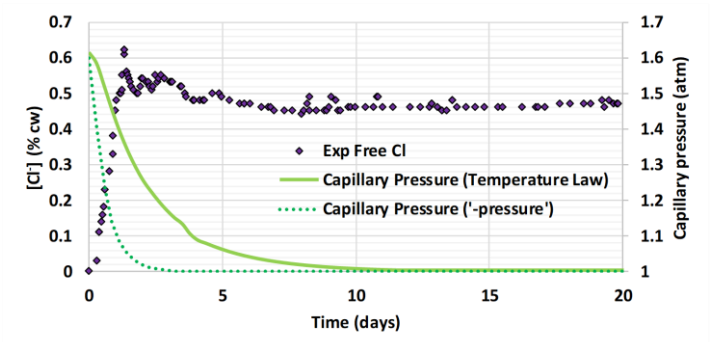

(a) Evolution of the capillary pressure in the porosity at 20 mm with the PhreeqC's routine 'pressure' and with the temperature law used later in this paper

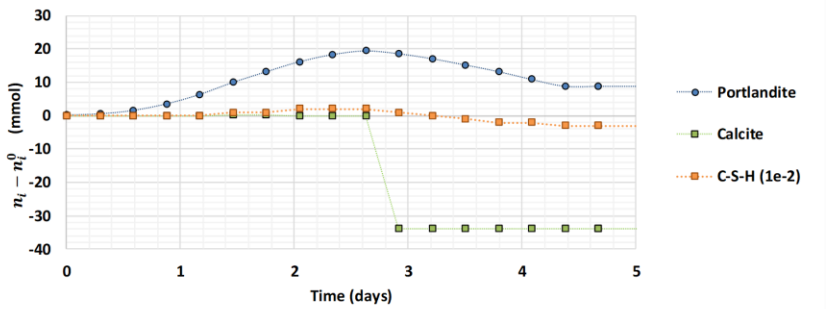

(b) Evolution of Portlandite, Calcite and C3AH6 contents at 20 mm

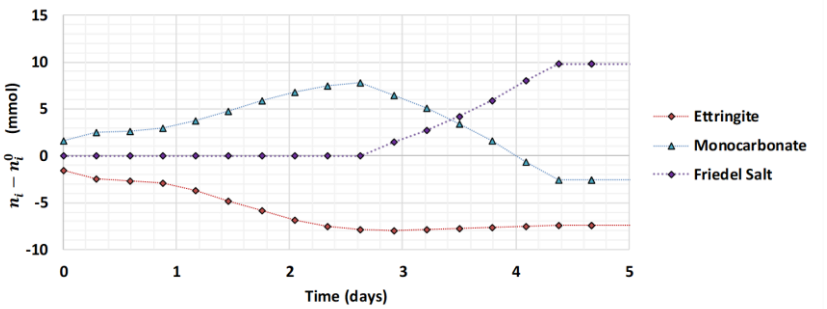

(c) Evolution of C-S-H, Ettringite, Monocarbonate and Friedel salts contents at 20 mm

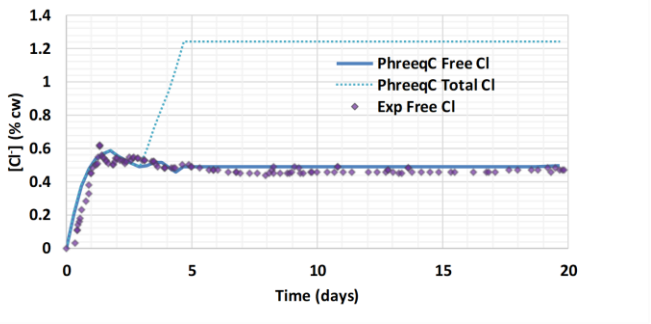

(d) Evolution of the free and total chloride at 20 mm

Figure 8. PhreeqC simulation with Advection-Dispersion model considering the capillary pressure effect

Finally, all those analyses with the PhreeqC simulations allow to better understand the processes involved during the capillary test. A satisfactory prediction of the chloride evolution measured by the OF sensor was achieved assuming the following hypothesis (Figure 9):

(i) 0-24 hours: A simple Advection-Dispersion transport (calibrated with the water velocity v_{H2O} and the microstructure geometry α_L) allowed the water to saturate the pore microstructure;

(ii) 1-7 days: The capillary pressure decreased enough to enable chemical reactions: mainly the AFm dissolution to create Friedel salts with chloride ions;

(iii) 7-20 days: As water has just saturated the material porosity, the diffusion transport replaced the Advection-Dispersion. The free and total chloride will respectively reach 1.02 % and 0.62 % of cement weight after 120 days and 450 days.

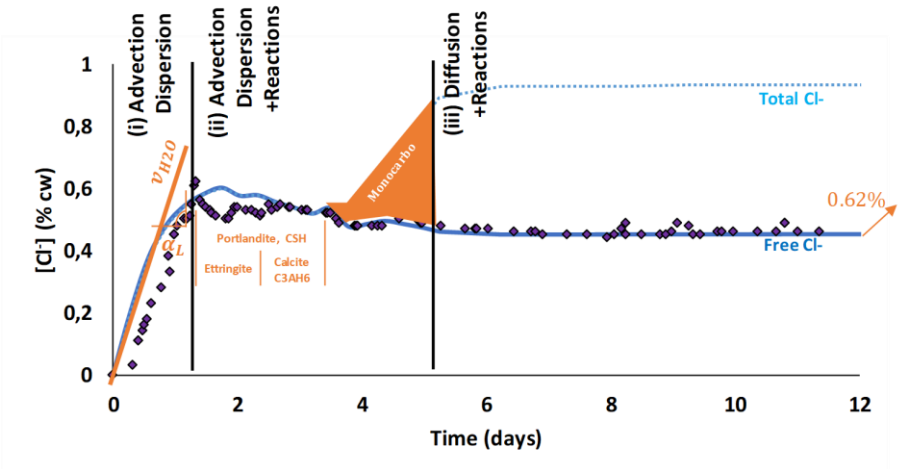

Figure 9. Explanation of the different processes involved during the capillarity tests according to the PhreeqC simulations.

5 CONCLUSIONS

A new chloride sensor with optical fiber technology was previously developed to measure the evolution of the chloride concentration in the pore solution in a cementitious material. Such sensor is a promising non-destructive remote monitoring tool for the health and the maintenance of concrete structures. The ingress of free chloride in the pore solution of a concrete sample during capillarity tests was simulated using the prediction model TransChlor. Although it seemed to give a good approximation of the chloride transport

through the material, some differences between the simulation and the measurements during the first few hours made it difficult to explain all the processes involved.

The original contribution of this work is twofold:

(i) To apply a latest developed OF sensor to finely measure the chloride concentration evolution in time during a capillary absorption test of a dried concrete sample in contact with salt-rich water;

(ii) To apply a step-by-step model to understand the main phenomena occurring during a capillary transport of chloride ions through a partially saturated concrete.

The capillarity test measurement data have then been broken down in order to identify all the different steps and expose the influence of the capillary pressure. First, the water saturated the pore microstructure by an advection-dispersion mechanism and the capillary pressure made chemical reactions negligible. Then, chloride ions were adsorbed by the cement matrix as the capillary pressure decreased. At last, the water ended up saturating the material porosity then a diffusion transport replaced the advection-dispersion.

Some further predictions estimate that the free chloride content in the pore solution will increase and reach the maximal value (0.62 % of cement weight) after 60 days of test. Those predictions were only possible through a complete understanding of the chloride transport mechanisms in structures submitted to the capillary suction.

The combination of the remote monitoring sensor with the numerical prediction model could improve the prediction of the structural behaviour without having to carry out destructive testing.

ACKNOWLEDGEMENTS

The authors would like to acknowledge the financial support obtained from the Natural Sciences and Engineering Council of Canada, Canada Foundation for Innovation, Advanced materials research and innovation hub, Hydro-Québec and Polycor inc.

REFERENCES

[1] F. Pruckner, Corrosion and protection of reinforcement in concrete measurements and interpretation, na, 2001.

[2] S. Qian, D. Cusson, Electrochemical evaluation of the performance of corrosion-inhibiting systems in concrete bridges, Cem. Concr. Compos. 26 (2004) 217–233.

[3] D. Cusson, B. Isgor, Durability of concrete structures: prevention, evaluation, inspection, repair and prediction, Can. Civ. Eng. 21 (2004) 4–5.

[4] A.M. Vaysburd, P.H. Emmons, Visible and invisible problems of concrete repair., Indian Concr. J. 75 (2001) 17–24.

[5] A.J. McPadden, Fiber optic corrosion and chloride sensors, PhD Thesis, University of Vermont, 1996.

[6] F. Laferrière, Capteur chimique à fibres optiques pour la mesure des ions chlore dans le béton à un stade précoce, EPFL, 2005.

[7] K. Tuutti, Corrosion of steel in concrete, Swedish cement and concrete research institute, Rep. Fo. 4 (1982) 82.

[8] O. Klinghoffer, T. Frølund, E. Poulsen, Rebar corrosion rate measurements for service life estimates, in: ACI Fall Conv., 2000.

[9] N. Singh, S.C. Jain, A.K. Aggarwal, M.L. Singla, M. Singh, Simple fiber-optic technique for in-situ corrosion sensing in structures, in: Nondestruct. Eval. Aging Mater. Compos. IV, International Society for Optics and Photonics, 2000: pp. 201–206.

[10] R. Sorensen, B. Buhr, S. Rostam, Sensoring corrosion, Concr. Eng. Int. 6 (2002) 53–56.

[11] D. Inaudi, Fiber optic sensor network for the monitoring of civil engineering structures, PhD Thesis, Verlag nicht ermittelbar, 1997.

[12] B. Glišić, D. Inaudi, Fibre optic methods for structural health monitoring, John Wiley & Sons, Chichester, West Sussex, England ; Hoboken, NJ, 2007.

[13] P. Rochette, Capteurs a fibre optique integres a des materiaux composites pour le genie civil: Essais et simulations sur eprouvettes cruciformes (French text)., (2003).

[14] N. Uwira, N. Opitz, D.W. Lübbers, Influence of enzyme concentration and thickness of the enzyme layer on the calibration curve of the continuously measuring glucose optode, in: Oxyg. Transp. Tissue-V, Springer, 1984: pp. 913–921.

[15] X. Outhier, Les Capteurs à Fibres Optiques, Rapp. Maîtrise Paris. 7 (1997).

[16] F. Laferrière, D. Inaudi, P. Kronenberg, I.F.C. Smith, A new system for early chloride detection in concrete, Smart Mater. Struct. 17 (2008) 045017. https://doi.org/10.1088/0964-1726/17/4/045017.

[17] D. Conciatori, F. Laferrière, E. Brühwiler, Comprehensive modeling of chloride ion and water ingress into concrete considering thermal and carbonation state for real climate, Cem. Concr. Res. 40 (2010) 109–118. https://doi.org/10/bd9q4n.

[18] D. Conciatori, H. Sadouki, E. Brühwiler, Capillary suction and diffusion model for chloride ingress into concrete, Cem. Concr. Res. 38 (2008) 1401–1408. https://doi.org/10/b3gvv4.

[19] D. Conciatori, E. Denarié, E. Brühwiler, Influence of microclimate on the probability of initiation of chloride induced corrosion in reinforced concrete, in: 4th Int. PhD Symp. Civ. Eng., Munich, Germany, 2002: p. 7p.

[20] T. Luping, L.-O. Nilsson, Chloride binding capacity and binding isotherms of OPC pastes and mortars, Cem. Concr. Res. 23 (1993) 247–253.

[21] D. Conciatori, E. Brühwiler, R. Gysler, Brine absorption in concrete at low temperature: Experimental investigation and modeling, J. Mater. Civ. Eng. 23 (2010) 846–851. https://doi.org/10/fwgg7p.

[22] D. Conciatori, Effet du microclimat sur l" initiation de la corrosion des aciers d" armature dans les ouvrages en béton armé, Thèse de doctorat, École Polytechnique Fédérale de Lausanne, 2006.

[23] C. Sachs, A new generation of sensors-Optodes, in: Ann. Biol. Clin. (Paris), JOHN LIBBEY EUROTEXT LTD 127 AVE DE LA REPUBLIQUE, 92120 MONTROUGE, FRANCE, 1999: pp. 107–107.

[24] G. Boisdé, A. Harmer, Chemical and biochemical sensing with optical fibers and waveguides, Artech House Publishers, 1996.

[25] E.A. Mendoza, R.A. Lieberman, D.P. Robinson, Sol-gel-based fiber optic and integrated optic chemical sensors for environmental monitoring and process control, in: Sol-Gel Opt. IV, International Society for Optics and Photonics, 1997: pp. 267–275. https://doi.org/10.1117/12.290203.

[26] A. Dybko, W. Wroblewski, J. Maciejewski, R.S. Romaniuk, Z. Brzozka, Fiber optic probe for monitoring of drinking water, in: Chem. Biochem. Environ. Fiber Sens. IX, International Society for Optics and Photonics, 1997: pp. 361–367. https://doi.org/10.1117/12.276172.

[27] W. Skoog, D.M. West, Holler, Fundam. Anal. Chem. (1997).

[28] J.R. Albani, Absorption et fluorescence, (2001).

[29] O.S. Wolfbeis, Fluorescence Spectroscopy: New Methods and Applications, Springer Science & Business Media, 2012.

[30] M. Probes, Fluorescent indicators for chloride-product information, (2001).

[31] J. Biwersi, B. Tulk, A.S. Verkman, Long-Wavelength Chloride-Sensitive Fluorescent Indicators, Anal. Biochem. 219 (1994) 139–143. https://doi.org/10.1006/abio.1994.1242.

[32] M.M.J. Oosthuizen, M.E. Englbrecht, H. Lambrechts, D. Greyling, R.D. Levy, The effect of pH on chemiluminescence of different probes exposed to superoxide and singlet oxygen generators, J. Biolumin. Chemilumin. 12 (1997) 277–284. https://doi.org/10.1002/(SICI)1099-1271(199711/12)12:6<277::AID-BIO455>3.0.CO;2-B.

[33] C. Huber, I. Klimant, C. Krause, T. Werner, T. Mayr, O.S. Wolfbeis, Optical sensor for seawater salinity, Fresenius J. Anal. Chem. 368 (2000) 196–202. https://doi.org/10.1007/s002160000493.

[34] F. Wissing, J.A.C. Smith, Vacuolar Chloride Transport in Mesembryanthemum crystallinum L. Measured Using the Fluorescent Dye Lucigenin, J. Membr. Biol. 177 (2000) 199–208. https://doi.org/10.1007/s002320010003.

[35] A. Lobnik, M. Čajlaković, Sol–gel based optical sensor for continuous determination of dissolved hydrogen peroxide, Sens. Actuators B Chem. 74 (2001) 194–199. https://doi.org/10.1016/S0925-4005(00)00733-4.

[36] D.L. Parkhurst, C.A.J. Appelo, Description of input and examples for PHREEQC version 3–A computer program for speciation, batch-reaction, one-dimensional transport, and inverse geochemical calculations, (2013).

[37] D.L. Parkhurst, C.A.J. Appelo, User's guide to PHREEQC (Version 2): A computer program for speciation, batch-reaction, one-dimensional transport, and inverse geochemical calculations, (1999).

[38] C.A.J. Appelo, L.R. Van Loon, P. Wersin, Multicomponent diffusion of a suite of tracers (HTO, Cl, Br, I, Na, Sr, Cs) in a single sample of Opalinus Clay, Geochim. Cosmochim. Acta. 74 (2010) 1201–1219. https://doi.org/10.1016/j.gca.2009.11.013.

[39] J.G. Charney, R. Fjörtoft, J. von Neumann, Numerical integration of the barotropic vorticity equation, Tellus. 2 (1950) 237–254.

[40] C.D. Shackelford, D.E. Daniel, Diffusion in saturated soil. I: Background, J. Geotech. Eng. 117 (1991) 467–484.

[41] G.T. Yeh, V.S. Tripathi, A critical evaluation of recent developments in hydrogeochemical transport models of reactive multichemical components, Water Resour. Res. 25 (1989) 93–108.

[42] E. Fehlberg, Low-order classical Runge-Kutta formulas with stepsize control and their application to some heat transfer problems, (1969).

[43] J. Raphson, Analysis aequationum universalis seu ad aequationes algebraicas resolvendas methodus generalis, & expedita, ex nova infinitarum serierum methodo, deducta ac demonstrata, typis Tho. Braddyll, prostant venales apud Johannem Taylor, 1702.

[44] E. Denarié, D. Conciatori, E. Brühwiler, Effect of microclimate on chloride penetration into reinforced concrete, in: Thessaloniki, Greece, 2003: p. 21 p.

[45] Z.P. Bažant, L.J. Najjar, Drying of concrete as a nonlinear diffusion problem, Cem. Concr. Res. 1 (1971) 461–473.

[46] P. Lunk, G. Mayer, Einfluss des Eindringens von Chloriden auf die wartungsfreie Nutzungsdauer von Stahlbetontragwerken, (1998).

[47] D. Conciatori, E. Brühwiler, Sub-zero transport: low temperature capillary tests in concrete, in: 2nd Int. RILEM Symp. Adv. Concr. Sci. Eng. Publ. Inf. Quebec City Can. Cds Publ., 2006.

[48] H. Freundlich, Über die Adsorption in Lösungen, Z. Für Phys. Chem. 57U (1907) 385–470. https://doi.org/10.1515/zpch-1907-5723.

[49] J. Provete Vincler, T. Sanchez, V. Turgeon, D. Conciatori, L. Sorelli, A modified accelerated chloride migration tests for UHPC and UHPFRC with PVA and steel fibers, Cem. Concr. Res. 117 (2019) 38–44. https://doi.org/10.1016/j.cemconres.2018.12.006.

[50] D.A. Kulik, T. Wagner, S.V. Dmytrieva, G. Kosakowski, F.F. Hingerl, K.V. Chudnenko, U.R. Berner, GEM-Selektor geochemical modeling package: revised algorithm and GEMS3K numerical kernel for coupled simulation codes, Comput. Geosci. 17 (2013) 1–24. https://doi.org/10.1007/s10596-012-9310-6.

[51] W. Hummel, U. Berner, E. Curti, F.J. Pearson, T. Thoenen, Nagra/PSI chemical thermodynamic data base 01/01, Radiochim. Acta. 90 (2002) 805–813.

[52] B. Lothenbach, F. Winnefeld, Thermodynamic modelling of the hydration of Portland cement, Cem. Concr. Res. 36 (2006) 209–226. https://doi.org/10.1016/j.cemconres.2005.03.001.

[53] E. Giffaut, M. Grivé, Ph. Blanc, Ph. Vieillard, E. Colàs, H. Gailhanou, S. Gaboreau, N. Marty, B. Madé, L. Duro, Andra thermodynamic database for performance assessment: ThermoChimie, Appl. Geochem. 49 (2014) 225–236. https://doi.org/10/f6n339.

[54] P. Blanc, P. Vieillard, H. Gailhanou, S. Gaboreau, N. Marty, F. Claret, B. Madé, E. Giffaut, ThermoChimie database developments in the framework of cement/clay interactions, Appl. Geochem. 55 (2015) 95–107. https://doi.org/10/f66gvq.

[55] U.A. Birnin-Yauri, F.P. Glasser, Friedel's salt, Ca2Al(OH)6(Cl,OH)·2H2O: its solid solutions and their role in chloride binding, Cem. Concr. Res. 28 (1998) 1713–1723. https://doi.org/10.1016/S0008-8846(98)00162-8.

[56] T. Matschei, B. Lothenbach, F.P. Glasser, The AFm phase in Portland cement, Cem. Concr. Res. 37 (2007) 118–130. https://doi.org/10.1016/j.cemconres.2006.10.010.

[57] A.J. Babchin, B. Faybishenko, On the capillary pressure function in porous media based on relative permeabilities of two immiscible fluids, Colloids Surf. Physicochem. Eng. Asp. 462 (2014) 225–230. https://doi.org/10.1016/j.colsurfa.2014.09.005.

[58] G. De Marsily, Quantitative hydrogeology, Paris School of Mines, Fontainebleau, 1986.

[59] H. Viallis-Terrisse, A. Nonat, J.-C. Petit, Zeta-Potential Study of Calcium Silicate Hydrates Interacting with Alkaline Cations, J. Colloid Interface Sci. 244 (2001) 58–65. https://doi.org/10/c7ccdw.

[60] Sanchez T., Henocq P., Aït-Mokhtar K., Millet O., Conciatori D., Chloride Diffusion in Cement Materials at Different Leaching States: An Experimental and Numerical Study, Cold Reg. Eng. 2019. (n.d.) 466–474. https://doi.org/10.1061/9780784482599.054.

[61] J. Olmeda, P. Henocq, E. Giffaut, M. Grivé, Modelling of chemical degradation of blended cement-based materials by leaching cycles with Callovo-Oxfordian porewater, Phys. Chem. Earth Parts ABC. 99 (2017) 110–120. https://doi.org/10/gbk5qt.